Excited State Intramolecular Proton Transfer in Schiff Bases. Decay of the Locally Excited Enol State Observed by Femtosecond Resolved Fluorescence

William Rodríguez-Córdoba, Jimena S. Zugazagoitia, Elisa Collado-Fregoso, and Jorge Peon*

Instituto de Química, Universidad Nacional Autónoma de México, Ciudad Universitaria, 04510, México, D.F., México

Received: March 27, 2007; In Final Form: May 15, 2007

Although the late ($t > 1$ ps) photoisomerization steps in Schiff bases have been described in good detail, some aspects of the ultrafast (sub-100 fs) proton transfer process, including the possible existence of an energy barrier, still require experimental assessment. In this contribution we present femtosecond fluorescence up-conversion studies to characterize the excited state enol to cis-keto tautomerization through measurements of the transient molecular emission. Salicylideneaniline and salicylidene-1-naphthylamine were examined in acetonitrile solutions. We have resolved sub-100 fs and sub-0.5 ps emission components which are attributed to the decay of the locally excited enol form and to vibrationally excited states as they transit to the relaxed cis-keto species in the first electronically excited state. From the early spectral evolution, the lack of a deuterium isotope effect, and the kinetics measured with different amounts of excess vibrational energy, it is concluded that the intramolecular proton transfer in the S_1 surface occurs as a barrierless process where the initial wave packet evolves in a repulsive potential toward the cis-keto form in a time scale of about 50 fs. The absence of an energy barrier suggests the participation of normal modes which modulate the donor to acceptor distance, thus reducing the potential energy during the intramolecular proton transfer.

Introduction

Due to their photochromism and intramolecular hydrogen bonding, Schiff bases are some of the most important compounds in photochemistry.[1−8] The excited state intramolecular proton transfer (ESIPT) present in these compounds makes them also interesting case studies for theoretical studies of molecular dynamics in electronically excited states. One of the most frequently studied photochromic Schiff bases is 2-((phenylimino)methyl)phenol (salicylideneaniline = SA). The general pathway of the photochromism in SA and similar Schiff bases is as follows:[9−28] The basal enol form is excited to a ($\pi-\pi^*$) state from where the hydroxylic proton is quickly transferred to the nitrogen imino atom; the resulting geometry corresponds to the fluorescent cis-keto tautomer (also a ($\pi-\pi^*$) state) which may undergo relaxation toward a ground state trans-keto isomer form (photochromic tautomer). Since the decay of the excited enol state is very fast, the steady state emission from these compounds is dominated by the cis-keto tautomer which has fluorescence lifetimes of up to a few tens of picoseconds.[15,18,19,23,29]

The development of ultrafast spectroscopic techniques has allowed the direct observation of proton transfer dynamics in several molecular systems.[30−45] Thanks to these techniques, several details of the photochemistry of the Schiff bases have come to view in the past few years. The most recent transient absorption study on SA was performed by the group of Ziólek,[19] where it was observed that the transient absorption and stimulated emission signals assigned to the cis-keto form appear within their time resolution of 50 fs. In agreement with previous studies,[9,10,14−16,29] these signals decay with a time constant of 6.8 ± 1.1 ps in acetonitrile solution (absorption for $\lambda < 530$ nm and stimulated emission for $\lambda > 530$ nm). Long-lived ($t \gg 1$ ns) residual transient absorbance around 480 nm due to the photochromic tautomer was also detected.

The 50 fs time scale for proton transfer is consistent with recent laser induced fluorescence experiments on jet cooled SA,[10] where the large homogeneous broadening observed in the excitation spectrum is a signature of the fast depletion of the ($\pi-\pi^*$) enol state. Additional aspects about the electronically excited states of SA come from a theoretical study and from femtosecond-resolved resonance enhanced multiphoton ionization (REMPI) experiments.[9,46] The calculations of ref 46 indicate the presence of a singlet ($n-\pi^*$) state of the enol form near the spectroscopic ($\pi-\pi^*$) state, and the REMPI experiments have detected that, in the gas phase, this ($n-\pi^*$) state may be populated from the decay of the spectroscopic state in a time scale of less than a picosecond.[9]

Despite significant research on the SA molecule, some aspects of its ultrafast photochemistry still require investigation. For example, it remains unclear whether an energy barrier exists along the proton transfer reaction coordinate. In the theoretical study of ref 46 it was reported that, for the ESIPT in SA, a potential energy barrier exists and that the enol ($\pi-\pi^*$) state is a local minimum in this surface. At the CIS/6-31G(d) theory level, the activation energy was calculated to be 7.2 kcal/mol, while at the same transition state geometry the TD-DFT/B3LYP/6-31G(d) method predicted a much smaller energy barrier of 3.2 kcal/mol.[46] In order to characterize the proton transfer dynamics and to determine whether such an energy barrier exists, we have performed time-resolved-fluorescence up-conversion measurements of the parent compound SA and its analogue 2-((naphthalen-1-ylimino)methyl)phenol (salicylidene-1-naphthylamine = SN; see Scheme 1). To test the existence of an energy barrier for the proton transfer process, we performed experiments on the hydroxyl-deuterated forms of SA and SN at selected wavelengths. Additionally, we present

* Corresponding author. E-mail: jpeon@servidor.unam.mx.

10.1021/jp072415d CCC: $37.00
Published on Web 06/21/2007

SCHEME 1: Structures of the Schiff Bases in This Study

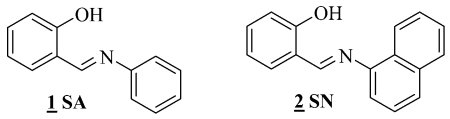

1 SA 2 SN

anisotropy measurements of the two compounds to observe if the evolution of the excited state during the proton transfer implies changes in the orientation of the emission transition dipole moment. Finally, for SN we include up-conversion measurements with two different excitation energies to determine the influence of the excess vibrational energy in the proton transfer dynamics.

Experimental Methods

Synthesis of Compounds 1 and 2: General Procedure. Equimolar solutions of the amines (1 mol) and 2-hydroxybenzaldehyde (1 mol) in dry ethanol (15 mL) were heated at reflux for 3 h. The ethanol was distilled off, and the residual was recrystallized twice from ethanol. Physical properties were confirmed from previous studies.[18,47,48] The ^{1}H NMR spectra were determined on a Bruker-Avance 300 MHz spectrometer in deuterochloroform with tretramethylsilane as internal standard. Data are reported as follows: chemical shifts (multiplicity, number of protons, coupling constants, and group).

*o-((Phenylimino)methyl)phenol (N-Salicylideneaniline) (**1**).* This compound was obtained in 87% yield as a yellow solid, mp 50−51 °C; δH (300 MHz, $CDCl_3$, Me_4Si), 13.20 (s, 1H, OH), 8.63 (s, 1H, CH═N), 7.45−7.25 (m, 7H, ArH), 7.04 (d, 1H, J = 7.65 Hz, ArH), 6.94 (dt, 1H, J = 7.48, 1.12 Hz, ArH).

*2-((Naphthalen-1-ylimino)methyl)phenol (Salicylidene-1-naphthylamine) (**2**).* This compound was obtained in 75% yield as a yellowish brown solid. δH (300 MHz, $CDCl_3$, Me_4Si) 13.35 (s, 1H, OH), 8.73 (s, 1H, HC═N), 8.28−8.23 (m, 1H, ArH), 7.92−7.86 (m, 1H, ArH), 7.81 (d, 1H, J = 8.30 Hz, ArH), 7.60−7.42 (m, 5H, ArH), 7.22 (dd, 1H, J = 7.31, 0.92 Hz, ArH), 7.15 (d, 1H, J = 8.22 Hz, ArH), 7.00 (dt, 1H, J = 7.49, 1.07 Hz, ArH).

General Procedure for the Deuteration of SA and SN. The solutions of SA and SN in dry CD_3OD were introduced in a closed system equipped with a mechanical stirrer and a constant flux of dry N_2. After 7 h of vigorous stirring and the vacuum evaporation of the solvent, the deuterated compounds at the hydroxyl groups were obtained. The absence of the hydroxyl proton signal (13.20 ppm) in the ^{1}H NMR spectrum of the deuterated SA indicated that deuterium exchange had occurred. The ^{1}H NMR spectrum of SN presents a very broad and weak signal for the hydroxyl proton due to the fast exchangeability between the oxygen and nitrogen atoms. For the deuterated SN sample, this broad feature is not observed. To confirm the isotope substitution in SA and SN, ^{2}H NMR spectra were measured. The single ^{2}H signal observed at the respective chemical shifts for SA and SN confirmed the nearly quantitative deuteration process.

Steady State and Time-Resolved Spectroscopy. All measurements were performed at room temperature (20 ± 1 °C) in HPLC-quality acetonitrile (Aldrich). The stationary absorption and the steady state fluorescence emission and excitation spectra were taken in a 1 cm quartz cell with Cary-50 and Cary Eclipse spectrophotometers (Varian), respectively.

Our femtosecond fluorescence up-conversion setup has been described in detail elsewhere.[49] It is based on a Ti:sapphire oscillator pumped by a 5 W, Verdi V5 laser (Coherent Inc.). The 100 MHz femtosecond pulse train was passed through a fused silica prism compressor before it was frequency doubled in a 0.5 mm BBO crystal. The second harmonic was separated from the remaining fundamental and its polarization adjusted with a half-wave plate before it was focused into a 1 mm path length flow cell containing the sample. The average power at the sample was 5 mW, and the focused spot was about 0.1 mm in diameter. The fluorescence was collected and refocused with a pair of parabolic mirrors, and at the focal point, it was crossed at another 0.5 mm BBO crystal with a vertically polarized, focused, and temporally delayed gate pulse from the remaining fundamental. The resulting sum frequency mixing signal was then focused to the entrance slit of a 10 cm focal length double monochromator (Oriel) and detected with a photomultiplier tube. The time resolution for our apparatus was measured through a cross-correlation scheme between the gate pulses and the Raman scattering of the pump beam in acetonitrile using the same flow cell. The instrument response function (IRF) was determined to have a 180 ± 10 fs full width at half-maximum (fwhm) for the experiments with 385 nm excitation, and 210 ± 10 fs for the experiments with 415 nm excitation.

Up-conversion traces were modeled as multiexponential decays analytically convoluted with the instrument function. The errors in the exponential time constants are approximately 20% for the sub-100 fs components and less than 10% otherwise. These errors are estimated from the time constants obtained from different data sets of the same experiment. With our signal-to-noise ratio, we estimate that, after deconvolution, the shortest decay time constant which can be resolved is 40 fs (see data for SN at 490 and 505 nm). From numerical simulations of the convoluted signals, we observed that time constants below this number cannot be reliably determined since they cannot be distinguished from a 40 fs decay time. Time-resolved emission spectra were measured at concentrations of 6.0×10^{-3} M for SA and 2.4×10^{-3} M for SN to obtain the absorbance of 0.4 and 1.2, respectively, at the pump wavelength. The influence of the concentration was checked in the 3.0×10^{-4}−6.0×10^{-3} M range for SA and SN, and no changes in the shape of the stationary absorption spectra were observed. For the experiments with deuterated samples, anhydrous acetonitrile was used and the solutions were kept isolated from air by flowing dry N_2 through the solution during the experiments. Through runs with the solvent only, we verified that the signals are not contaminated with up-conversion of the Raman scattering by the solvent or the cell.

Results

The steady state absorption, emission, and excitation spectra of acetonitrile solutions of SA and SN are shown in Figures 1 and 2. Previous studies of both compounds have established that, in this solvent, the tautomer responsible for the ground state absorption is the hydrogen-bonded enolic form and that the first band with significant oscillator strength corresponds to a ($\pi-\pi^*$) transition, with maxima at 337 nm for SA and 350 nm for SN.[18,19,36] The prominent bands in the fluorescence spectra of both compounds show large Stokes shifts of 11 051 cm^{-1} for SA (λ_{max} = 537 nm) and 10 289 cm^{-1} for SN (λ_{max} = 547 nm). In both cases, the principal band corresponds to emission from the cis-keto tautomer formed after photoinduced proton transfer.[14−16,18,19,23] In both figures it is clear that, apart from the main band, a small amount of fluorescence is detected in the range of 400−520 nm. The weak, short-wavelength emission has been associated with emitting species which precede the appearance of the fluorescent cis-keto tau-

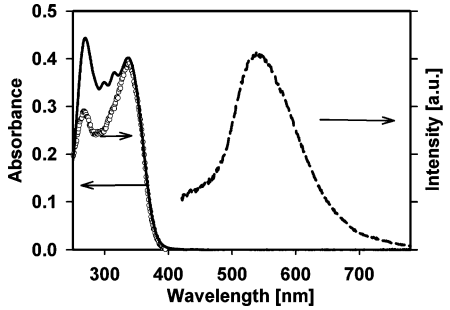

Figure 1. Absorption (continuous line), emission (dashed line), and excitation (circles) spectra of SA in acetonitrile solution. The fluorescence spectra were taken with an excitation wavelength of 360 nm. The excitation spectra were taken by measuring the emission at 570 nm.

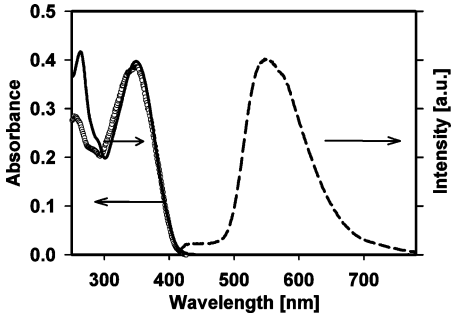

Figure 2. Absorption (continuous line), emission (dashed line), and excitation (circles) spectra of SN in acetonitrile solution. The fluorescence spectra were taken with an excitation wavelength of 360 nm. The excitation spectra were taken by measuring the emission at 570 nm.

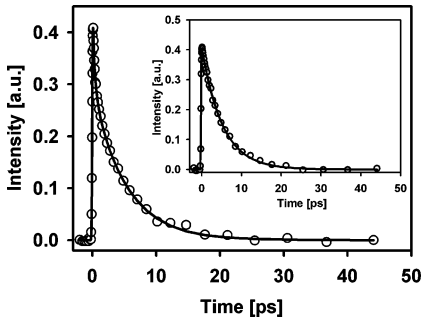

Figure 3. Fluorescence up-conversion measurements of SA in acetonitrile solution in the tens of picoseconds time range. The excitation wavelength was 385 nm, and the fluorescence was detected at 510 (main) and 605 nm (inset). Solid lines are convoluted multiexponential fits to the data.

tomer.[14,15,19] The femtosecond resolution of the emission in this region is the main focus of this paper.

In Figures 3−6 we show frequency up-conversion results of the two compounds including several traces taken in the short-wavelength side of the cis-keto band. These figures correspond to experiments using an excitation wavelength of 385 nm. For both Schiff bases it was observed that the emission decays in multiple time scales which range from sub-100 fs to several picoseconds with different contributions across the emission spectrum. In Figures 3 (SA) and 4 (SN), we show up-conversion traces in the time range of several tens of picoseconds for two representative wavelengths. Preliminary analysis of the data as multiexponential decays and also trial fits considering only times longer than 1 ps showed that practically the same decay time constant is observed (within a 0.5 ps difference) for $t > 1$ ps in the entire spectral region from 490 to 640 nm. These "long" decay times are 5.2 ± 0.5 ps for SA and 20 ± 1 ps for SN.

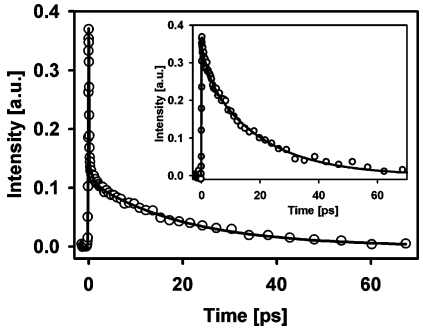

Figure 4. Fluorescence up-conversion measurements of SN in acetonitrile solution in the tens of picoseconds time range. The excitation wavelength was 385 nm, and the fluorescence was detected at 525 (main) and 625 nm (inset). Solid lines are convoluted multiexponential fits to the data.

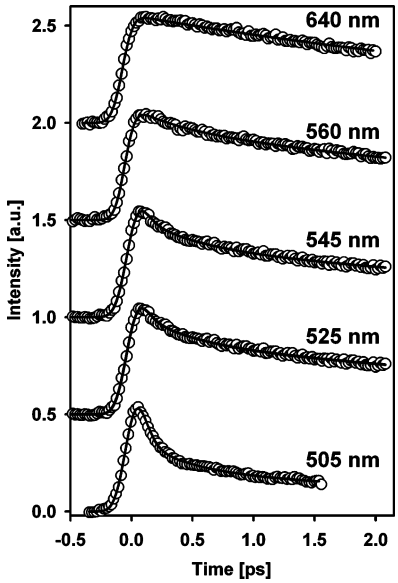

Figure 5. Fluorescence up-conversion measurements of SA in acetonitrile solution in the short time range. The excitation wavelength was 385 nm. Solid lines are global fits to multiexponential decays convoluted with the instrument response function.

Such a fluorescence component in the picosecond range has been previously attributed to the S_1 ($\pi-\pi^*$) state of the cis-keto tautomer which decays due to conversion to the ground state and, to some extent, the formation of photochromic forms (ground state conformers of the keto tautomer). Our cis-keto S_1 state lifetime of 5.2 ps in acetonitrile compares very well with the 6.7 ± 1.5 ps lifetime obtained by Ziólek et al. through time-correlated single photon counting with a resolution of about 1 ps.[19]

Once the time constant of the longest decay component was established, the full time range of the up-conversion experiments was fitted using a global nonlinear least-squares scheme. The data were modeled with three exponentially decaying terms analytically convoluted with the instrument response function. The global fits were made constraining the time constants to have the same (global) values for all the fluorescence wavelengths and allowing the amplitudes of the three decaying terms to vary freely. In particular, the longest time constant was fixed at the values determined from the procedure described previously (5.2 and 20 ps, respectively).

The results of the multiexponential analysis are summarized in Table 1. For SA we observed emission decays with time constants of $\tau_1 = 50$ fs, $\tau_2 = 430$ fs, and $\tau_3 = 5.2$ ps. The contribution of the 50 fs component is most prominent (up to

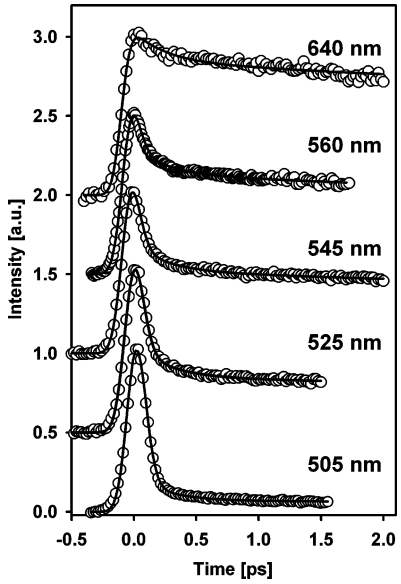

Figure 6. Fluorescence up-conversion measurements of SN in acetonitrile solution in the short time range. The excitation wavelength was 385 nm. Solid lines are global fits to multiexponential decays convoluted with the instrument response function.

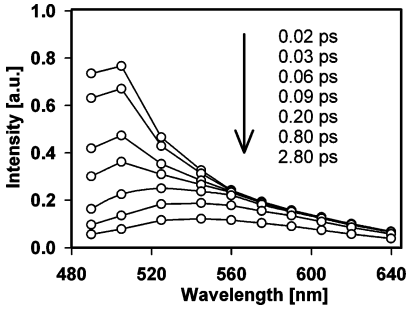

Figure 7. Time-resolved emission spectra for SA in acetonitrile solution. Excitation wavelength: 385 nm.

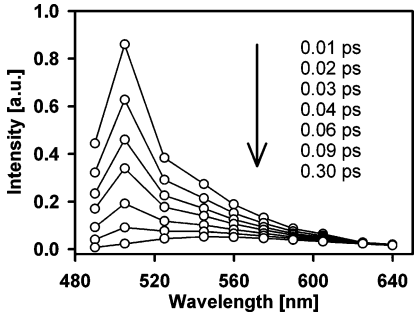

Figure 8. Time-resolved emission spectra for SN in acetonitrile solution. Excitation wavelength: 385 nm.

80% of the total decay) for the short-wavelength side of the steady state emission spectrum. For the experiments detecting at 560 and 575 nm, the data were satisfactorily described maintaining only the 430 fs and 5.2 ps components, and for wavelengths ≥590 nm, the data may be described with a single exponential. In particular, for the data at 640 nm, we observed that the signal is also consistent with a small rise with a time constant of 40 fs with about 15% of the amplitude of the decaying component. This exercise showed that, with our time resolution, a small rising component at 640 nm cannot be ruled out.

Similarly, for SN the time constants were $\tau_1 \leq 40$ fs, $\tau_2 = 270$ fs, and $\tau_3 = 20$ ps. The 40 fs component should be taken as an upper limit due to our time resolution. All three components are important to describe the data for wavelengths up to 605 nm, while for the fluorescence at 625 and 640 nm the data could be fitted by keeping only the two longer exponentials. In this case, the data are inconsistent with rising terms for all the wavelengths. The spectral evolution which takes place during the first picoseconds after photoexcitation was determined by calculating the time-resolved emission spectra (TRES) using a scaling procedure with the single wavelength traces and the steady state spectra.[50] The TRES for SA and SN are included in Figures 7 and 8.

In order to study the femtosecond evolution of the relative orientation of the excitation and the emission transition dipole moments during the proton transfer and relaxation processes, we have measured the fluorescence anisotropy of the SA and SN solutions after excitation with 385 nm pulses. The anisotropy was determined at the short- (505 nm) and long- (640 nm) wavelength sides of the fluorescence spectra, and the results are shown in Figures 9 and 10 for SA and SN, respectively.

TABLE 1: Multiexponential Decay Parameters Obtained for the Fluorescence Decay of SA and SN in Acetonitrile Solution

	SN ($\lambda_{exc} = 385$ nm)			SA ($\lambda_{exc} = 385$ nm)		
λ_{fluo} (nm)	α_1	α_2	α_3	α_1	α_2	α_3
490	98	1	1	82	9	9
505	96	2	1	74	13	13
525	88	5	7	49	15	35
545	82	5	13	27	15	58
560	74	7	19		19	81
575	67	6	27		9	91
590	56	8	36			100
605	50	10	40			100
625		26	74			100
640		24	76			100

	SN-d_1 ($\lambda_{exc} = 385$ nm)			SA-d_1 ($\lambda_{exc} = 385$ nm)		
λ_{fluo} (nm)	α_1	α_2	α_3	α_1	α_2	α_3
490	98	1	1	82	9	9

	SN ($\lambda_{exc} = 415$ nm)					
λ_{fluo} (nm)	τ_1 (ps)	τ_2 (ps)	τ_3 (ps)	α_1	α_2	α_3
505	0.05	0.49	20	92	3	5
525	0.05	0.29	20	78	7	15
560		0.08	20		59	41

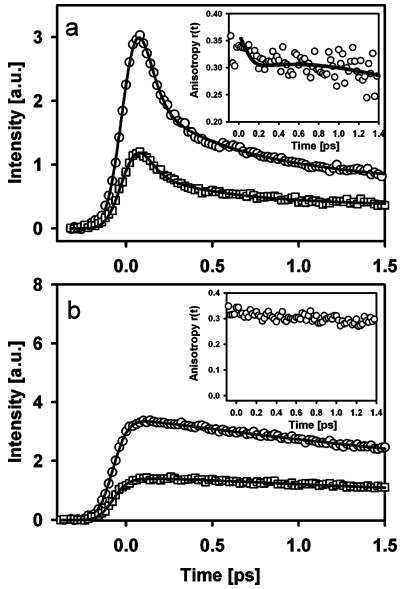

Figure 9. Main graphs: Femtosecond fluorescence up-conversion measurements of SA in acetonitrile solution taken with parallel (circles) and perpendicular (squares) excitation−detection configurations. In (a) the fluorescence wavelength was 505 nm, and in (b) it was 640 nm. The excitation wavelength was 385 nm. The insets show anisotropy values calculated from the two experimental traces.

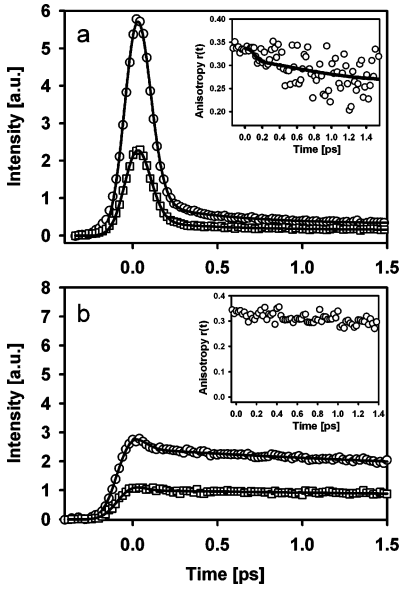

Figure 10. Main graphs: Femtosecond fluorescence up-conversion measurements of SN in acetonitrile solution taken with parallel (circles) and perpendicular (squares) excitation−detection configurations. In (a) the fluorescence wavelength was 505 nm, and in (b) it was 640 nm. The excitation wavelength was 385 nm. The insets show anisotropy values calculated from the two experimental traces.

The emission anisotropy as a function of time was calculated according to $r(t) = (I_{||} - I_{\perp})/(I_{||} + 2I_{\perp})$. This was evaluated directly from the up-conversion data taken with parallel ($I_{||}$) and perpendicular ($I_{\perp}$) excitation−detection configurations (circles in the insets). Additionally, for the data sets at 505 nm, the anisotropy was determined from the deconvoluted multiexponential functions obtained from fits to $I_{||}$ and $I_{\perp}$, and corresponds to the solid lines in the insets. These graphs show that for both SA and SN the anisotropy near $t = 0$ has a value of about 0.34 at both wavelengths. The anisotropy shows only a minimal rapid change in the first 100 fs (see continuous lines at 505 nm) due to the enol to cis-keto geometry change. After this small modulation, $r(t)$ decays on a much slower time scale due to rotational diffusion of the fluorescent cis-keto state. From single-exponential fits, the anistotropy decay times due to rotational relaxation are approximately 11 ps for SA and 16 ps for SN in acetonitrile.

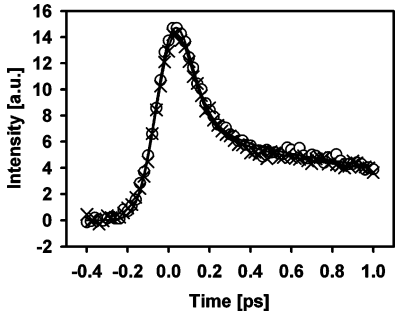

Figure 11. Femtosecond fluorescence up-conversion measurements of SA (circles) and deuterated SA (crosses) in acetonitrile solution. The excitation wavelength was 385 nm, and the detected fluorescence wavelength was 490 nm. The solid lines are fits to multiexponential decays convoluted with the instrument response function.

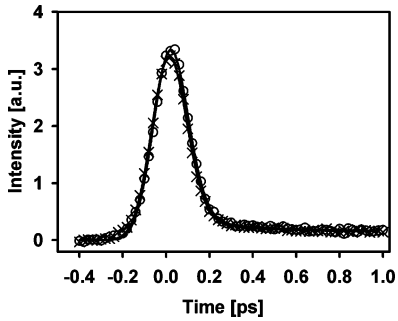

Figure 12. Femtosecond fluorescence up-conversion measurements of SN (circles) and deuterated SN (crosses) in acetonitrile solution. The excitation wavelength was 385 nm, and the fluorescence wavelength was 490 nm. The solid lines are fits to multiexponential decays convoluted with the instrument response function.

We also determined the effect of deuteration on the decay times in the short-wavelength side of the fluorescence spectrum. The femtosecond up-conversion measurements of deuterium-exchanged SA and SN in acetonitrile solutions (SA-d_1 and SN-d_1) at the fluorescence wavelength of 490 nm were taken in back-to-back experiments with the respective nondeuterated solutions of SA and SN. This was done to avoid any small changes in the instrument response function of the apparatus which might occur with day-to-day operation. The results are shown in Figures 11 (SA, SA-d_1) and 12 (SN, SN-d_1). As can be seen from the raw data, there is no change in the traces taken with the deuterated Schiff bases in comparison with the regular solutions and the time constants and amplitudes are well inside the uncertainties of the measurements. The small differences in the amplitudes of the signals at their maximums are due to small differences in the concentrations of the solutions. From these experiments it can be immediately concluded that deuteration has no effect on the multiexponential decay observed in the short-wavelength region of the emission. Since at this wavelength the emission is dominated by the precursors of the cis-keto S_1 state, the absence of a deuterium isotope effect speaks about a proton transfer without the involvement of a potential energy barrier.[51−54]

Finally, several of the up-conversion measurements were repeated for SN, now using an excitation wavelength of 415 nm. While vertical excitation at 385 nm places the SN molecule in an enol-type geometry with an energy 5975 cm^{-1} (0.74 eV)

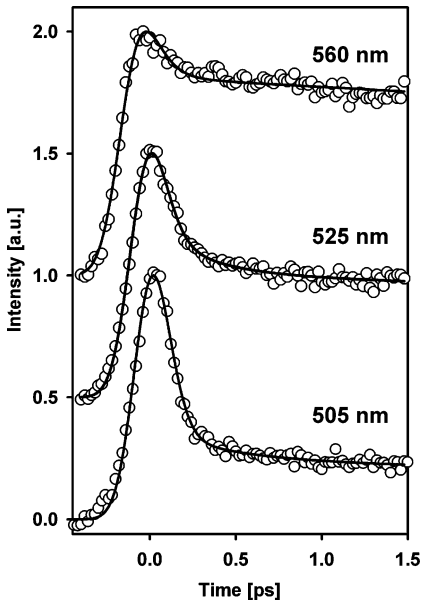

Figure 13. Fluorescence up-conversion measurements of SN in acetonitrile solution in the short time range. The excitation wavelength was 415 nm. Solid lines are global fits to multiexponential decays convoluted with the instrument response function.

above the 0−0 transition for the cis-keto emission (low-wavelength edge of the keto emission: 500 nm), excitation at 415 nm changes this excess energy to 4096 cm^{-1} (0.51 eV), that is, a 0.23 eV difference. The results of these experiments are included in Table 1 and Figure 13. As can be seen, even with the excitation wavelength of 415 nm, which is at the edge of the absorption spectrum of SN (at the 0−0 transition for the enol geometry), the signals in the short-wavelength side (505 nm) are still dominated by an ultrafast component of $\tau_1 \approx 50$ fs with a more than 90% amplitude in the multiexponential decay. This behavior is indicative of a proton transfer process whose mechanism is insensitive to the excess vibrational energy in the first excited state.

Discussion

Ultrafast Decay in the Short-Wavelength Region and Spectral Evolution. Previous studies on Schiff bases have used the transient absorption technique to determine the proton transfer dynamics.[14−16,36−38] In particular, SA in acetonitrile solution was most recently studied by the group of Ziólek.[19] There, the IRF-limited rise times of signals assigned to the cis-keto tautomer were used to estimate an upper limit of 50 fs for the proton transfer. It is likely that, due to an overlap with the $S_1 \rightarrow S_n$ transient absorption bands of the ($\pi-\pi^*$) cis-keto state, those experiments were unable to detect transient absorption decays which could be attributed to the precursor of the cis-keto state. Our experiments, which resolve the molecular emission with a more appropriate time resolution than previous fluorescence measurements, do not suffer from such band crowding, and the early sub-100 fs and subpicosecond decays are well resolved. From the spectral region where the ultrafast short-wavelength emission occurs and in agreement with ref 19, we attribute the sub-100 fs signals to the rapid depopulation of the precursor of the cis-keto species, that is, the fast motion of the vibrational wave packet away from the enol geometry. The time scale for this type of proton transfer is dictated by the frequency of vibrational modes which are able to modulate the donor-to-acceptor distance, thereby reducing the potential energy along the proton transfer coordinate.[34,35,55−57] The participation of such low-frequency modes has been identified from the oscillatory behavior of transient absorption signals and correspond to in-plane deformations in molecules like 2-(2′-hydroxyphenylbenzooxazole (HBO). The geometry of SA in the enol ground state corresponds to a nonplanar structure since the anilino ring makes a dihedral angle of about 49° with the rest of the molecule.[10,46,47] Despite this structural difference with molecules like HBO, which is planar,[58] it appears that similar modes which reduce the oxygen-to-nitrogen distance exist and determine the proton transfer rate. It should be mentioned that the gas-phase REMPI experiments of ref 9 determined that the SA proton transfer time was lower than 750 fs. Our results, in agreement with those from the Ziólek group, establish that in solution the fluorescent cis-keto tautomer can be formed in a much shorter time scale of about 50 fs, a time scale similar to other intramolecular proton transfer systems.[19,34,35,55−57]

The second exponential component of the signals (270 fs for SN and 430 for SA) is attributed to the vibrational energy redistribution and cooling which occurs after the proton transfer event. This time scale is in agreement with recent UV-pump, IR-probe experiments which examined the vibrational relaxation which occurs immediately after UV-induced proton transfer in 2-(2′-hydroxyphenyl)benzothiazole.[55]

The anisotropy measurements in these two molecules clearly show that the orientation between the transition dipole directions (absorption vs emission) practically does not change when the molecular emission shifts toward longer wavelengths as the proton transfer and vibrational relaxation take place. This result is evidence that the change in aromaticity involved in the photoexcitation (which actually drives proton transfer[51]) is established from the early times (sub-50 fs) and throughout the lifetime of the cis-keto S_1 state, indicating that the progress along the proton transfer coordinate is similar to the motion of a vibrational wave packet in a repulsive potential energy surface.

Deuteration and Excess Vibrational Energy Effects. A common test for the existence of energy barriers in reactions which involve hydrogen is the observation of a kinetic deuterium isotope effect.[52−54] Semiclassical treatments predict significant increases in reaction times when the proton is replaced by deuterium if quantum tunneling is responsible for the reaction or if the reaction is thermally activated.[51,59] Our experiments conclusively show that, for both Schiff bases SA and SN, there are no changes in the short-wavelength emission decays upon deuteration, even for excitation at the 0−0 transition of the enol absorption band (385 nm for SA and 415 nm for SN). This result is in disagreement with the theoretical calculations at the CIS/6-31G(d) level which calculated a transition state energy of 7.2 kcal/mol above the $S_1(\pi-\pi^*)$ enol geometry.[46] In that same article it was indicated that, at the same transition state geometry, use of a TD/B3LYP/6-31G(d) method lowers the energy barrier to 3.2 kcal/mol. A more recent TD-DFT study about the ESIPT in a similar Schiff base, salicylidene methylamine (SMA), determined that the energy profile along the reaction coordinate in this molecule does not involve a barrier and that there is no local energy minimum at the enol geometry in this electronic state.[60] Our results indicate that the reaction profile in SA and SN is more consistent with this picture of a direct proton transfer process. The qualitative differences between the SMA theoretical results and the calculations of ref 46 are probably related to the different computational methodologies. In particular, the geometry of the transition state in ref 46 was determined at the CIS/6-31G(d) level, while in ref 60 this was achieved through the TD/B3LYP/6-31G(d,p) method.

Further evidence that the proton transfer occurs without an energy barrier comes from the comparison of the ultrafast decays between excitation with 385 nm (3.22 eV) and excitation with 415 nm (2.99 eV) pulses. The results in Figures 6 and 13 show that the ultrafast decay of the short-wavelength emission of SN is maintained even when the electronic excitation is made with near-zero vibrational energy for the enol geometry. That is, since the shape of the potential energy surface of the electronically excited enol form makes the molecule evolve directly as a vibrational wave packet toward the cis-keto geometry (without a barrier), the amount of vibrational energy has a minimal effect in the decay of the emission assigned to the enol S_1 state "in transit" (cis-keto precursor).

Conclusions

We have resolved the ultrafast emission from the precursor of the excited cis-keto tautomer of SA and SN in acetonitrile solutions. Although the molecule at the locally excited enol-like geometry is highly fluorescent, its short lifetime determines the small contribution it makes to the steady state emission spectrum. From the early spectral evolution, the absence of a deuterium isotope effect, and the dominance of sub-100 fs components, even with excitation at the edge of the enol absorption spectrum, we conclude that the prompt dynamic process involves a vibrational wave packet which evolves along the proton transfer coordinate and disappears in the time scale a few vibrational periods. The relaxed cis-keto geometry is attained within the first picosecond through the combination of intramolecular vibrational redistribution and cooling which is likely mediated by large-amplitude vibrations.

Acknowledgment. We are thankful to Professor Ahmed H. Zewail and the California Institute of Technology for the donation of equipment used in this study. For financial support we are thankful to Consejo Nacional de Ciencia y Tecnología (CONACyT, Grant 42663Q), and to Universidad Nacional Autónoma de México (UNAM, direct funding from the University Rector office). We wish to thank M. C. Nieves Zavala Segovia for the acquisition of the proton and deuterium NMR spectra of SA and SN.

References and Notes

(1) Amimoto, K.; Kawato, T. *J. Photochem. Photobiol., C* **2005**, *6*, 207.
(2) Padwa, A. *Chem. Rev.* **1977**, *77*, 37.
(3) Gilli, P.; Bertolasi, V.; Pretto, L.; Lycka, A.; Gilli, G. *J. Am. Chem. Soc.* **2002**, *124*, 13554.
(4) Potashnik, R.; Ottolenghi, M. *J. Chem. Phys.* **1969**, *51*, 3671.
(5) Richey, W. F.; Becker, R. S. *J. Chem. Phys.* **1968**, *49*, 2092.
(6) Irie, M.; Mohri, M. *J. Org. Chem.* **1988**, *53*, 803.
(7) Yokoyama, Y. *Chem. Rev.* **2000**, *100*, 1717.
(8) Benniston, A. C. *Chem. Soc. Rev.* **2004**, *33*, 573.
(9) Okabe, C.; Nakabayashi, T.; Inokuchi, Y.; Nishi, N.; Sekiya, H. *J. Chem. Phys.* **2004**, *121*, 9436.
(10) Otsubo, N.; Okabe, C.; Mori, H.; Sakota, K.; Amimoto, K.; Kawato, T.; Sekiya, H. *J. Photochem. Photobiol., A* **2002**, *154*, 33.
(11) Becker, R. S.; Richey, W. F. *J. Am. Chem. Soc.* **1967**, *89*, 1298.
(12) Fujiwara, T.; Harada, J.; Ogawa, K. *J. Phys. Chem. B* **2004**, *108*, 4035.
(13) Ogawa, K.; Harada, J.; Fujiwara, T.; Yoshida, S. *J. Phys. Chem. A* **2001**, *105*, 3425.
(14) Mitra, S.; Tamai, N. *Chem. Phys.* **1999**, *246*, 463.
(15) Mitra, S.; Tamai, N. *Phys. Chem. Chem. Phys.* **2003**, *5*, 4647.
(16) Mitra, S.; Tamai, N. *Chem. Phys. Lett.* **1998**, *282*, 391.
(17) Becker, R. S.; Lenoble, C.; Zein, A. *J. Phys. Chem.* **1987**, *91*, 3509.
(18) Ohshima, A.; Momotake, A.; Arai, T. *J. Photochem. Photobiol., A* **2004**, *162*, 473.
(19) Ziólek, M.; Kubicki, J.; Maciejewski, A.; Naskrecki, R.; Grabowska, A. *Phys. Chem. Chem. Phys.* **2004**, *6*, 4682.
(20) Joshi, H.; Kamounah, F. S.; Gooijer, C.; van der Zwan, G.; Antonov, L. *J. Photochem. Photobiol., A* **2002**, *152*, 183.
(21) Sekikawa, T.; Kobayashi, T.; Inabe, T. *J. Phys. Chem. B* **1997**, *101*, 10645.
(22) Sekikawa, T.; Kobayashi, T.; Inabe, T. *J. Phys. Chem. A* **1997**, *101*, 644.
(23) Barbara, P. F.; Rentzepis, P. M.; Brus, L. E. *J. Am. Chem. Soc.* **1980**, *102*, 2786.
(24) Barbara, P. F.; Brus, L. E.; Rentzepis, P. M. *J. Am. Chem. Soc.* **1980**, *102*, 5631.
(25) Rospenk, M.; Krol-Starzomska, I.; Filarowski, A.; Koll, A. *Chem. Phys.* **2003**, *287*, 113.
(26) Kownacki, K.; Mordzinski, A.; Wilbrandt, R.; Grabowska, A. *Chem. Phys. Lett.* **1994**, *227*, 270.
(27) Grabowska, A.; Kownacki, K.; Kaczmarek, L. *J. Lumin.* **1994**, *60/61*, 886.
(28) Knyazhansky, M. I.; Metelitsa, A. V.; Kletskii, M. E.; Millov, A. A.; Besugliy, S. O. *J. Mol. Struct.* **2000**, *526*, 65.
(29) Vargas, V. *J. Phys. Chem. A* **2004**, *108*, 281.
(30) Lärmer, F.; Elsässer, T.; Kaiser, W. *Chem. Phys. Lett.* **1988**, *148*, 119.
(31) Wiechmann, M.; Port, H.; Lärmer, F.; Frey, W.; Elsässer, T. *Chem. Phys. Lett.* **1990**, *165*, 28.
(32) Wiechmann, M.; Port, H.; Frey, W.; Lärmer, F.; Elsässer, T. *J. Phys. Chem.* **1991**, *95*, 1918.
(33) Zhong, D.; Douhal, A.; Zewail, A. H. *Proc. Natl. Acad. Sci. U.S.A.* **2000**, *97*, 14056.
(34) Lochbrunner, S.; Stock, K.; Riedle, E. *J. Mol. Struct.* **2004**, *700*, 13.
(35) Lochbrunner, S.; Stock, K.; Riedle, E. *J. Chem. Phys.* **2000**, *112*, 10699.
(36) Ziólek, M.; Kubicki, J.; Maciejewski, A.; Naskrecki, R.; Grabowska, A. *J. Chem. Phys.* **2006**, *124*, 124518.
(37) Ziólek, M.; Kubicki, J.; Maciejewski, A.; Naskrecki, R.; Grabowska, A. *J. Photochem. Photobiol., A* **2006**, *180*, 101.
(38) Ziólek, M.; Kubicki, J.; Maciejewski, A.; Naskrecki, R.; Grabowska, A. *Chem. Phys. Lett.* **2003**, *369*, 80.
(39) Kobayashi, T.; Sekikawa, T.; Inabe, T. *J. Lumin.* **1997**, *72*, 508.
(40) Nakagaki, R.; Kobayashi, T.; Nakamura, J.; Nagakura, S. *Bull. Chem. Soc. Jpn.* **1977**, *50*, 1909.
(41) Higelin, D.; Sixl, H. *Chem. Phys.* **1983**, *77*, 391.
(42) Turbeville, W.; Dutta, P. K. *J. Phys. Chem.* **1990**, *94*, 4060.
(43) Yuzawa, T.; Takahashi, H.; Hamaguchi, H. *Chem. Phys. Lett.* **1993**, *202*, 221.
(44) Knyazhansky, M. I.; Metelitsa, A. V.; Bushkov, A. J.; Aldoshin, S. M. *J. Photochem. Photobiol., A* **1996**, *97*, 121.
(45) Mandal, A.; Fitzmaurice, D.; Waghorne, E.; Koll, A.; Filarowski, A.; Guha, D.; Mukherjee, S. *J. Photochem. Photobiol., A* **2002**, *153*, 67.
(46) Zgierski, M. Z.; Grabowska, A. *J. Chem. Phys.* **2000**, *112*, 6329.
(47) Destro, R.; Gavezotti, A.; Simonetta, M. *Acta Crystallogr.* **1978**, *B34*, 2867.
(48) Simion, A.; Simion, C.; Kanda, T.; Nagashima, S.; Mitoma, Y.; Yamada, T.; Mimura, K.; Tashiro, M. *J. Chem. Soc., Perkin Trans. 1* **2001**, 2071−2078.
(49) Morales-Cueto, R.; Esquivelzeta-Rabell, M.; Saucedo-Zugazagoitia, J.; Peon, J. *J. Phys. Chem. A* **2007**, *111*, 552.
(50) Lakowicz, J. R. *Principles of fluorescence spectroscopy*, 2nd ed.; Kluwer Academic/Plenum: New York, 1999.
(51) Douhal, A.; Lahmani, F.; Zewail, A. H. *Chem. Phys.* **1996**, *207*, 477.
(52) Herek, J. L.; Pedersen, L.; Bañares, L.; Zewail, A. H. *J. Chem. Phys.* **1992**, *97*, 9046.
(53) Frey, W.; Lärmer, F.; Elsässer, T. *J. Phys. Chem.* **1991**, *95*, 10391.
(54) Schwartz, B. J.; Peteanu, L. A.; Harris, C. B. *J. Phys. Chem.* **1992**, *96*, 3591.
(55) Rini, M.; Dreyer, J.; Nibbering, E. T. J.; Elsässer, T. *Chem. Phys. Lett.* **2003**, *374*, 13.
(56) Chudoba, C.; Riedle, E.; Pfeiffer, M.; Elsässer, T. *Chem. Phys. Lett.* **1996**, *263*, 622.
(57) Lochbrunner, S.; Szeghalmi, K.; Stock, K.; Schmitt, M. *J. Chem. Phys.* **2005**, *122*, 244315.
(58) Segala, M.; Domingues, N. S., Jr.; Livotto, R. P.; Stefan, V. *J. Chem. Soc., Perkin Trans. 2* **1999**, 1123.
(59) Arnaut, L. G.; Formosinho, S. J.; Barroso, M. *J. Mol. Struct.* **2006**, *786*, 207.
(60) Ortiz, J. M.; Gelabert, R.; Moreno, M.; Lluch, J. M. *J. Phys. Chem. A* **2006**, *110*, 4649.